**C.M. Cully · R.E. Ergun · K. Stevens ·
A. Nammari · J. Westfall**

The THEMIS Digital Fields Board

Abstract The Digital Fields Board (DFB) performs the data acquisition and signal processing for the Electric Fields Instrument and Search Coil Magnetometer on each of the THEMIS (Time History of Events and Macroscale Interactions during Substorms) satellites. The processing is highly flexible and low-power ($\sim$1.1 Watt orbit-averaged). The primary data products are time series waveforms and wave power spectra of the electric and magnetic fields. The power spectra can be computed either on the raw signals (i.e. in a system co-rotating with the spacecraft) or in a coordinate system aligned with the local DC magnetic field. Other data products include spectral power from multiple passbands (filter banks) and electric power in the 30kHz-500 kHz band. All five DFBs have been turned on and checked out in-flight, and are functioning perfectly.

Keywords THEMIS · signal processing · electric field instrument · search-coil magnetometer

PACS 07.50.Qx; 07.87.+v; 94.80.+g; 95.55.-n; 84.40.Ua

1 Introduction

Despite many advances in our understanding of the substorm process, there remain some fundamental open questions. Where and when does the onset occur? What physical processes are primarily responsible? How do the individual components of a substorm interact? What is the mechanism through which a substorm drives the aurora?

C.M. Cully, R.E. Ergun, K. Stevens, A. Nammari and J. Westfall
Laboratory for Atmospheric and Space Physics
University of Colorado
Boulder, CO, 80303, USA
E-mail: chris.cully@irfu.se

The THEMIS (Time History of Events and Macroscale Interactions during Substorms) mission has been built to help answer these and other questions. It is a five-satellite NASA medium-class explorer mission launched in February 2007 in conjunction with an extensive ground-based instrument array. A detailed description of the THEMIS mission can be found elsewhere in this issue [Angelopoulos, 2008].

Some of the most intriguing open questions concern the role of local processes in the current sheet. For example, which plasma instabilities disrupt the cross-tail current? Which instabilities lead to reconnection? How are they related? Resolving these questions will require good electric and magnetic field measurements well above DC.

Electric and magnetic fields are observed by three types of sensors on THEMIS. The Flux-Gate Magnetometer (FGM) [Auster et al, 2008, this issue] and Search-Coil Magnetometer (SCM) [Roux et al, 2008, this issue] measure the magnetic fields, while the Electric Fields Instrument (EFI) [Bonnell et al, 2008, this issue] measures electric fields. The DFB is responsible for acquiring and processing all of the signals from the EFI and SCM, including multi-rate digital filtering and spectral processing. A unique processing function allows the calculation of spectra in field-aligned coordinates.

To reduce power consumption, all of the digital processing is done by three Field Programmable Gate Arrays (FPGAs) without the aid of a dedicated digital signal processor. The orbit-averaged DFB power consumption is roughly 1.1 Watt, of which roughly 390 mW is devoted to the analog electronics.

This paper discusses the DFB in detail. The next section presents an overview of the DFB functionality. Sections 3 and 4 discuss the analog and digital electronics, while sections 5, 6 and 7 present the three main digital functions: digital filtering, power spectrum calculation and rotation to field-aligned coordinates. Section 8 lists all of the available data products.

2 Overview

Figure 1 gives a top-level overview of the DFB. There are sixteen analog signals available for sampling, as listed in table 1. The three SCM signals are filtered to remove aliasing to give the 3 signals we call SCMX, SCMY and SCMZ, while the six EFI signals similarly yield signals V1 to V6. The EFI signals from opposing sides of the spacecraft are also paired to give differential electric field measurements, which can be selected as either DC or AC coupled (E12, E34, E56, E12AC, E34AC and E56AC). Finally, there is one channel devoted to the high-frequency (50kHz-200 kHz) electric field (E12HF). These analog signals are converted and processed by the DFB, and the resulting digital products are sent to the Digital Control Board of the Instrument Data Processing Unit (IDPU) [Taylor et al, 2008].

To maximize the scientific output given the telemetry, the THEMIS mission makes extensive use of burst modes [Angelopoulos, 2008, this issue]. The lowest level of data collection, termed slow survey, covers the entire orbit at low resolution. The second level, termed fast survey, covers a relatively large fraction of the orbit at medium resolution. "Particle burst" covers a small
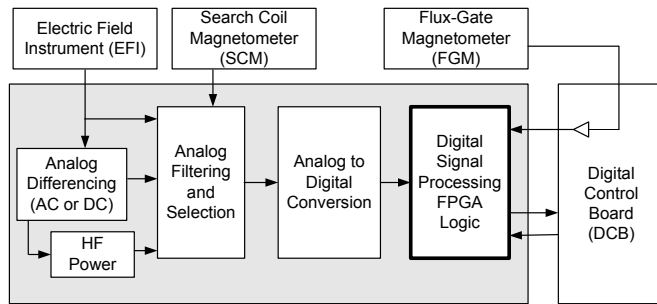
Fig. 1 Top-level schematic of DFB operation.

Table 1 Analog signals available for sampling

Mnemonic	Description
SCMX,SCMY,SCMZ	3-axis magnetic field from SCM
V1 to V6	Probe-spacecraft voltage for all 6 EFI sensors
E12,E34,E56	DC-coupled electric field from EFI
E12AC,E34AC,E56AC	AC-coupled electric field from EFI
E12HF	High frequency electric field from EFI

fraction of the orbit with high resolution particle and wave data, while the final "wave burst" level applies only to the EFI and SCM data, giving very high resolution data for short intervals. Data from higher-resolution burst levels do not interrupt the data flow from lower-resolution levels; for example, slow survey data is still collected when the satellite is in wave burst mode. Consequently, the DFB must produce a large number of data products tailored for the various burst levels.

3 Analog electronics

Nine signals arrive at the DFB input: 3 from the SCM and 6 from the EFI. All nine of these signals are available for sampling, as well as six differential signals for the EFI (Exx, ExxAC). Additionally, the power in the 50 kHz-200 kHz band is measured using a pseudo-logarithmic rectifying amplifier. Figure 2 shows the analog functionality.

Since the spacecraft voltage is typically much larger than the signal from the DC electric fields, the common mode rejection ratio for the differential amplifiers must be large. The DC common mode rejection ratio was tested on each board and is better than -80 dB. By precision matching capacitors, an AC common mode rejection ratio of better than -40 dB is attained over the full temperature range on all boards.

All signals are filtered to avoid aliasing. The EFI signals are filtered using 4-pole Bessel filters at either 4.0 kHz (for the 9 DC channels) or 8.0 kHz (for the 3 AC channels). The SCM signals are filtered using 4-pole Butterworth filters at 4.0 kHz.
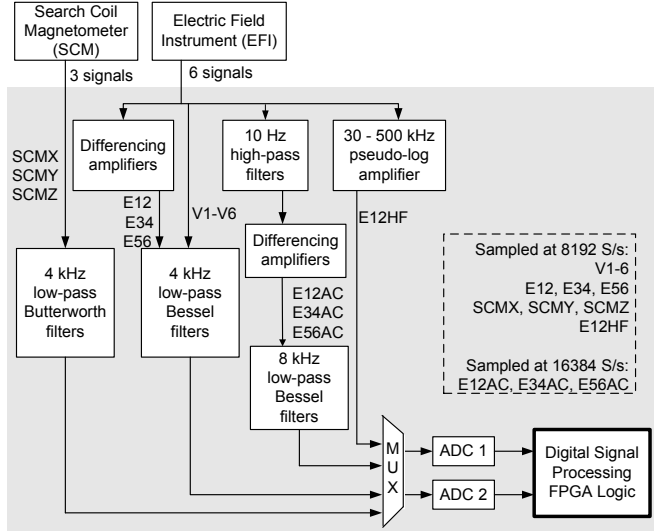
Fig. 2 Analog functionality.

To measure the power in the high-frequency electric field (E12HF), we use a 6-stage rectifying pseudo-logarithmic amplifier. Each stage is composed of a high-pass filter, a pair of clipping diodes and an amplifier with a gain of 5. The total amplification is $5^6 = 15625$, so that later amplifier stages easily (and intentionally) saturate. For larger input values, an increasing number of stages saturate, which gives the pseudo-logarithmic response seen in figure 3. The output from each of the six amplifier stages is half-wave rectified and summed before being low-pass filtered (1 pole, 500 Hz) to give the output signal. The frequency range matches the frequency range of auroral kilometric radiation (AKR) frequently seen at substorm onset.

All 16 analog signals are routed through a series of multiplexers to two redundant (cross-strapped) Linear Technologies LTC1604 analog to digital
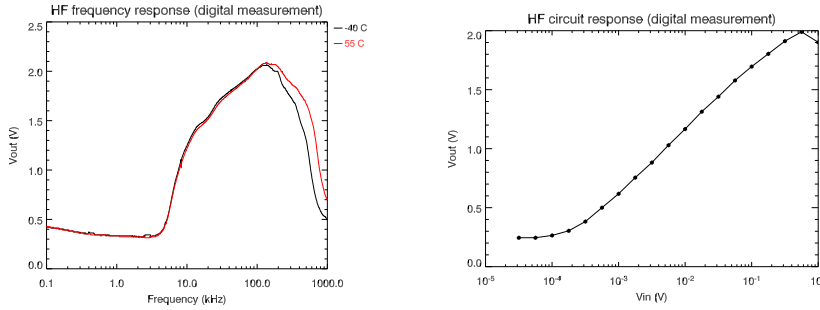

Fig. 3 E12HF response for board F6 (S/N 009); other units are similar. Left: output voltage as a function of frequency. Right: output voltage as a function of input voltage.

converters (ADCs). To save power, only signals that are actually needed for the telemetry are sampled, and the ADCs are put into a power-conserving nap mode whenever possible between samples. The worst-case crosstalk between channels is -81 dB, with most combinations considerably less than that.

4 Digital Electronics

The main component of the digital electronics is a set of three Actel RT54SX72S FPGAs that together function as an application-specific processor. These FP-GAs are triple-module redundant antifuse parts specifically made for space flight. We designed the FPGAs using VHDL (VHSIC (Very-High-Speed Integrated Circuit) Hardware Description Language), which allowed us to simulate the design in software during development, with full access to all internal signals.

One FPGA acts as the master controller. It is responsible for all external communications, runs the analog to digital converters and performs the digital filtering. The other two FPGAs are co-processing devices that calculate spectra and derived quantities. The clock to these two FPGAs can be shut down by the master FPGA to conserve power whenever their functionality is not required. All DFB functions are synchronized to a 1-Hz synchronization pulse provided by the IDPU in addition to the 8.4 MHz clock.

Internal bitwidth is carefully controlled to avoid roundoff or truncation errors. Any operations that could be subject to out-of-range numerical errors have been built to saturate cleanly and avoid wrap-around.

The three FPGAs share a common bank of 512 kb of RAM (random-access memory) arranged on a 32-bit bus. The RAM is radiation-hard (Honeywell HX6228TBRT), and memory access conflicts are handled by a fixed time-division multiplexed scheme.

5 Digital Filters

There are two main digital filtering functions: the bandpass filter banks and the lowpass waveform filtering. Both of these filtering operations are performed using the common filter bank architecture shown in figure 4.

The left half of figure 4 shows the first two levels of the low-pass filtering scheme. In the first level, the signal passes through two Finite Impulse Response (FIR) digital filters. The first FIR filter uses the function

$$y_n = a_1 x_n + a_2 x_{n-1} + a_3 x_{n-2} + a_4 x_{n-3} + a_5 x_{n-4} + a_6 x_{n-5} + a_7 x_{n-6} \tag{1}$$
$$a_{1..7} = \{-8, 0, 72, 128, 72, 0, -8\}/256 \tag{2}$$

where x_m is the input sequence and y_n is the output sequence. This filter operates as a low-pass filter at roughly 40% of the Nyquist frequency. As a FIR filter, the phase response is perfectly linear (i.e. equal group delay at all frequencies).
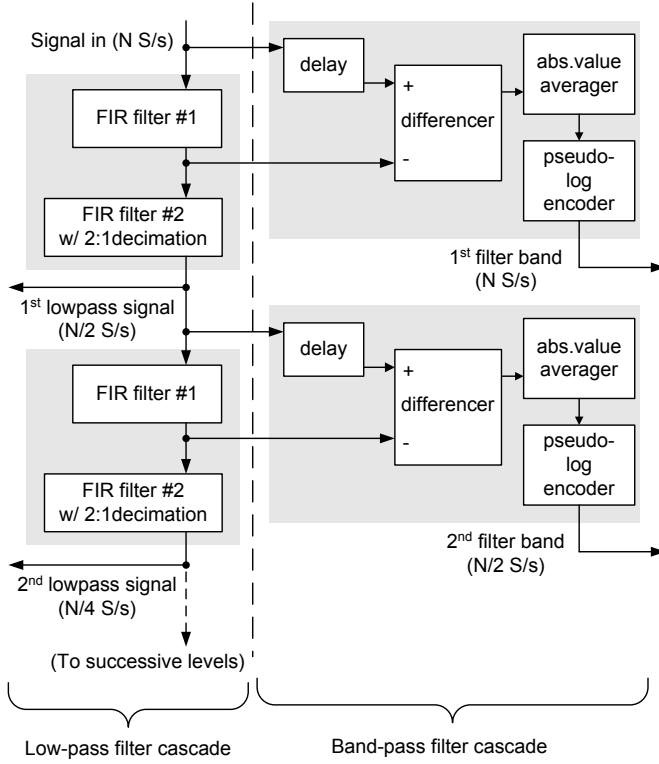
Fig. 4 Filter architecture.

The filter coefficients are chosen both to give a sharp filter cutoff and also to minimize resources in the FPGA. Since there are no built-in multipliers in the FPGAs, each multiply operation must be physically built up from the basic logic cells. By using coefficients that have only one or two non-zero bits in a binary representation, the multiplier can be constructed from simple shift operations, which greatly reduces complexity and logic usage.

The second filter is a decimating FIR filter. It uses the function

$$y_n = 0.25x_n + 0.5x_{n-1} + 0.25x_{n-2} \qquad (3)$$

but only keeps every second point. Consequently, the output rate is only half the input rate. The output of this filter forms the first level in the low-pass filter cascade.

This same filtering process is cascaded 12 times for most signals, and 13 times for the ExxAC signals (which are sampled at 16384 S/s rather than 8192 S/s). The result is a set of signals at every rate 2^n from 2 S/s up to 8192 S/s (16384 S/s for ExxAC). Since the rate decreases by a factor of 2 at each step, the computational resources required also decrease by a factor of 2 at each step. The full 12-step cascade therefore only requires about twice as much computation as the first step.
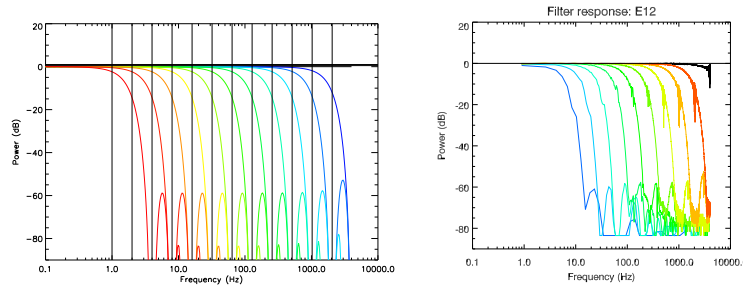
Fig. 5 Frequency response for the low-pass filter cascade. Left: predicted response. Right: response as measured on board F5 (S/N 007), channel E12. Artifacts at the Nyquist frequency are introduced by the test procedure and are not characteristic of the filters.
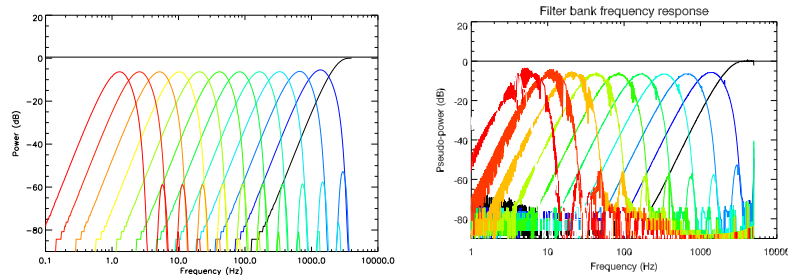

Fig. 6 Frequency response for the low-pass filter cascade. Left: predicted response. Right: response as measured on board F5 (S/N 007), channel E12. The raggedness in the test results below 100 Hz is an expected artifact of the swept-frequency test: the trigger quantities are reported at 16 S/s, which is over-sampled for the lowest frequencies.

Figure 5 shows the frequency response of the low-pass filter cascade as predicted (left) and as measured by sweeping a sine wave signal up to 4 kHz (right). The filter response is -13 dB at the Nyquist frequency, and falls at roughly 80 dB/octave from there. A side lobe occurs at roughly 3 times the Nyquist frequency, with a maximum amplitude of -59 dB.

For the bandpass signals, the filter cascade calculates the difference between the signal at each level before and after it passes through the first FIR filter in the lowpass cascade (see right hand side of figure 4). As a symmetric 7-tap filter, the FIR filter has a group delay of 3 points. Consequently, the unfiltered signal must be delayed by 3 points to avoid a phase mismatch. After differencing the two signals, the amplitude in the bandpass-filtered signal is estimated by taking the average of the absolute value. The amplitude is then compressed to 8 bits by a pseudo-logarithmic encoder.

The left hand panel of figure 6 shows the predicted frequency response of the bandpass-filtered signals. The highest-frequency signal is larger by a factor of 2, and similar sidelobes can be seen as in the lowpass filters. There is some jaggedness in the small-amplitude response, which is caused by the pseudo-logarithmic compression.

6 Derived Quantities

From a scientific perspective, electric and magnetic field spectra are more informative in a magnetic-field-aligned coordinate system. Thus, the DFB has the ability to rotate the observed 3D electric field magnetic fields signals into a field-aligned system before calculating the power spectra.

The parallel (to B) direction is uniquely specified. We take advantage of the fact that the perpendicular direction is not unique by selecting the signal that is both orthogonal to B and also in the spin plane. In this way, the perpendicular electric field signal is entirely derived from the spin-plane wire booms which have much lower noise and a well-defined gain. In the rare case that the spin axis is exactly parallel to B, a default direction is used.

On the ground, one could calculate the parallel and perpendicular components as

$$X_{||} \ = \ \frac{\mathbf{X} \cdot \mathbf{B}}{|\mathbf{B}|} \ = \ \frac{X_x B_x + X_y B_y + X_z B_z}{\sqrt{B_x^2 + B_y^2 + B_z^2}} \tag{4}$$

$$X_{\perp} = \frac{\mathbf{X} \times \mathbf{B}}{|\mathbf{B}|} = \frac{X_x B_y - X_y B_x}{\sqrt{B_x^2 + B_y^2 + B_z^2}} \tag{5}$$

where $\mathbf{X}$ is either the electric field from the EFI or the AC magnetic field from the SCM, and $\mathbf{B}$ is the DC magnetic field from the FGM. Although these operations could be performed by the FPGA, they are expensive in terms of FPGA logic (especially the square root), and we have devised a more efficient implementation.

The implementation relies on a method known as CORDIC (COordinate Rotation for DIgital Computers) [Volder, 1959; Andraka, 1998] that can arbitrarily rotate 2-dimensional vectors using minimal hardware resources. The DFB uses CORDIC both to rotate vectors for the derived quantities and also to calculate $\cos(\theta)$ for the Fast Fourier Transform calculations (see section 7).

The implementation we use in the DFB is sketched in figure 7. First, the CORDIC method is used to find the first two Euler angles required to rotate the FGM magnetic field vector onto the x-axis. These 2 rotations are about the z axis and the (rotated) y' axis, giving the 2 angles θ and ϕ. Next, the EFI and/or SCM data vectors are rotated through the same angles θ and ϕ (again using the CORDIC algorithm). The parallel and perpendicular components are then the x and y components in the rotated system.

The data is calibrated before the rotations occur. Variable offsets and gains are applied separately to the FGM data, the EFI data and the SCM data. These gains need to be computed on the ground and uploaded. For the EFI data, the offset can alternatively be calculated on-board using a 10-minute average. The FGM data are also rotated to align with the EFI or SCM coordinate system. The rotation operation is combined with the FGM gain into two 9-element rotation matrices: one for the EFI system and one for the SCM system.
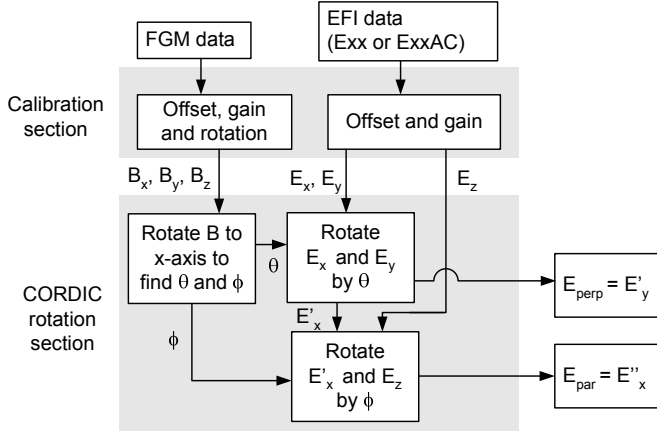
Fig. 7 Calculation of derived quantities $E_{||}$ and $E_{\perp}$. SCM quantities $\delta B_{||}$ and $\delta B_{\perp}$ are calculated similarly.

The FGM data arrive at the DFB in 24-bit precision at a rate of 128 S/s. To ensure synchronization, the EFI and/or SCM data are delayed to account for the full delay through the FGM chain to the DFB. The calculated angles θ and ϕ from the FGM vectors are then linearly interpolated in the DFB to avoid jumps in the coordinate system which would create noise at harmonics of 128 Hz.

The result of this processing is a set of four signals that we refer to as the "derived quantities". These four signals are the magnetic components $\delta B_{||}$ and $\delta B_{\perp}$ and the electric components $E_{||}$ and $E_{\perp}$. The electric components can be either AC-coupled (from ExxAC) or DC-coupled (Exx).

7 Calculation of Spectra

Power spectra are available in the particle burst and wave burst modes, and provide coverage for the higher frequency range. The spectra are computed by Fast Fourier Transforms (FFTs) implemented in the FPGAs. Figure 8 is a top-level flow diagram.
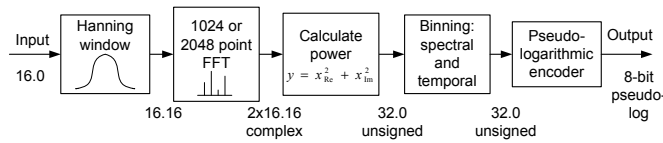

Fig. 8 Top-level flow diagram for FFT. Internal bitwidths are shown at each stage.

The DFB can calculate continuous FFTs of any four of 19 available signals: the 15 analog quantities in table 1 not including E12HF, plus the 4

derived signals discussed in section 6. 1024-point FFTs are used for all signals at 8192 S/s, while 2048-point FFTs are used for signals at 16384 S/s (ExxAC and any derived quantities using ExxAC). The resulting spectra are available at up to 8 spectra per second.

In order to optimize the use of FPGA resources, all operations are performed in a fixed-point format (not floating-point). The bitwidths of all internal signals were analyzed to ensure signal integrity; the resulting widths are shown in figure 8. The notation "16.16" means a 32-bit wide signed number, with 16 bits to the left of the decimal place and 16 bits to the right. By using a 32-bit internal representation, the resulting powers are identical with double-precision calculations to the level of $\sim$-95 dB.

We use a standard in-place decimation in time (Cooley-Tukey) algorithm for the FFT, with a Hanning window to reduce side lobes. To increase efficiency, the DFB packs two N-point real vectors into one N-point complex vector, processes the FFT for that one complex vector, and then unpacks the results appropriately [Press et al, 1992]. A CORDIC algorithm is used for the sine and cosine calculations.

In a fixed-point representation with no roundoff error, every multiplication doubles the bitwidth. In an FFT operation, this is not acceptable, since the bitwidth would geometrically grow with each butterfly operation. To avoid this, we clip the result of each butterfly pass to a 16.16 representation for each component (real and imaginary) and accept the small roundoff error. In the event of a rail-to-rail signal on the input, the maximum possible error with a pathological signal is -87 dB (3 bits). Using more reasonable signals, the maximum error is below the 1-bit floor (i.e. the calculated power is exact to the limit of its bitwidth).

After calculating the power from the complex FFT result, the DFB bins the spectral power in frequency and time according to the commanded mode. Binning in time is accomplished by averaging together spectra to reduce the cadence from the natural 8 spectra per second to as low as 1 spectra per 16 seconds. The number of combined spectra are 2^n with integral n. Frequency binning reduces the spectrum to either 16, 32 or 64 bins. Bin spacing is approximately logarithmic, as shown in tables 2 and 3. The lower frequency of each bin is equal to the sum of the bandwidths below it, starting from zero.

Table 2 Spectral binning for 1024-point FFT results

64-point spectra		32-point spectra		16-point spectra	
Bins	Bandwidth	Bins	Bandwidth	Bins	Bandwidth
0-31	8 Hz	0-15	16 Hz	0-7	32 Hz
32-39	32 Hz	16-19	64 Hz	8-9	128 Hz
40-47	64 Hz	20-23	128 Hz	10-11	256 Hz
48-55	128 Hz	24-27	256 Hz	12-13	512 Hz
56-63	256 Hz	28-31	512 Hz	14-15	1024 Hz

Table 3 Spectral binning for 2048-point FFT results

64-point spectra		32-point spectra		16-point spectra	
Bins	Bandwidth	Bins	Bandwidth	Bins	Bandwidth
0-15	8 Hz	0-7	16 Hz	0-3	32 Hz
16-23	16 Hz	8-11	32 Hz	4-5	64 Hz
24-31	32 Hz	12-15	64 Hz	6-7	128 Hz
32-39	64 Hz	16-19	128 Hz	8-9	256 Hz
40-47	128 Hz	20-23	256 Hz	10-11	512 Hz
48-55	256 Hz	24-27	512 Hz	12-13	1024 Hz
56-63	512 Hz	28-31	1024 Hz	14-15	2048 Hz

8 Data products and data rates

There are three basic types of data provided by the DFB: waveforms, filter bank data and spectra. Table 4 lists the available waveform data products, grouped by data ID and burst mode. All waveform data are 16 bits wide.

Table 4 Waveform data products (Data IDs in hexadecimal representation).

Data ID	Description	Burst mode	Quantities	Rate
450	Spin-fit data	slow survey	V1-4, E12, E34, E56	128 S/s
441	Voltage group A	fast survey	any V1-6	2-8192 S/s
442	Voltage group B	fast survey	any V1-6	2-8192 S/s
443	Electric field	fast survey	any Exx or ExxAC	2-16384 S/s
444	SCM data	fast survey	any SCM (X,Y,Z)	2-8192 S/s
445	Voltage group A	particle burst	any V1-6	2-8192 S/s
446	Voltage group B	particle burst	any V1-6	2-8192 S/s
447	Electric field	particle burst	any Exx or ExxAC	2-16384 S/s
448	SCM data	particle burst	any SCM (X,Y,Z)	2-8192 S/s
449	Voltage group A	wave burst	any V1-6	2-8192 S/s
44A	Voltage group B	wave burst	any V1-6	2-8192 S/s
44B	Electric field	wave burst	any Exx or ExxAC	2-16384 S/s
44C	SCM data	wave burst	any SCM (X,Y,Z)	2-8192 S/s

For slow survey, seven waveform signals (V1 through V4, E12, E34 and E56) at 128 S/s each are passed to the IDPU for spin fitting. The other data streams (IDs) can contain up to six different quantities at a single user-selectable rate of 2^n S/s (for integer n). Quantity and speed selection in the streams is entirely independent; for example, E12, E56 and E34AC could be grouped together on data ID 443 (hexadecimal), with E12 and E34 on data ID 447.

Filter bank data are 8 bits wide, and use a pseudo-logarithmic compression to attain a 19-bit range. The filter bank data types are listed in table 5. There are two output streams from the filter bank: one for slow survey data and one for input to the burst-mode triggering algorithm. The slow-survey filter bank data consist of 2 banks of 6 spectral bands each, covering the range from ~2 Hz to ~4 kHz with logarithmic spacing. Each bank may be set to any of the 16 input quantities except E12HF. The trigger data are

the same as the slow-survey data, except that 11 spectral bands are reported (instead of 6), and the rate is fixed at 16 S/s. Two additional quantities are included along with the filter bank quantities: the peak and average levels of the E12HF signal in the time period since the last filter bank data point.

Table 5 Filter bank data products

ID	Burst mode	Quantities	Bands	Rate
440	slow survey	any 2 of: V1-6, Exx, ExxAC, SCM	6	1/16-8 S/s
440	slow survey	E12HF: peak and average	-	same as above
451	trigger	same 2 quantities as ID 440	11	16 S/s
451	trigger	E12HF: peak and average	-	16 S/s

The -6 dB frequencies defining the filter passbands for 8192 Hz signals (i.e. all signals except ExxAC) are listed in table 6 as f_{min} and f_{max}. The appropriate frequencies for the 16 kS/s ExxAC signals are exactly twice these values. The frequency at which the filter response is maximized (f_{center}) and the total bandwidth (f_{max} - f_{min}) are also listed. The highest-frequency band is limited at high frequency only by the analog filters, and hence has an anomalously large bandwidth. In slow survey, filter levels 0,2,4,6,8 and 10 are included in the telemetry for 8 kS/s signals, and levels 1,3,5,7,9 and 11 are included for 16 kS/s signals, so that the passband frequencies remain similar.

Table 6 Filter bank passbands for 8 kS/s signals (double frequencies for 16 kS/s)

level	f_{min} (Hz)	f_{center} (Hz)	f_{max} (Hz)	bandwidth (Hz)
0	1390	2689	5994	4604
1	631	1149	1836	1204
2	316	572	904	587
3	159	287	453	293
4	80.2	144.2	227.4	147.2
5	40.2	72.3	113.9	73.7
6	20.1	36.2	57.0	36.9
7	10.1	18.1	28.5	18.4
8	5.04	9.05	14.26	9.23
9	2.52	4.53	7.13	4.61
10	1.26	2.26	3.57	2.31
11	0.63	1.13	1.78	1.15

Finally, the DFB computes the power spectral densities of any four signals from the set of the 15 analog quantities (table 1, not including E12HF) and the four derived quantities. Table 7 lists the spectral data available in particle and wave burst modes. The telemetry consists of either 16, 32 or 64 spectral power bands at a rate selectable from 1/16 S/s to 8 S/s. The bands cover the range up to 4 kHz in a roughly logarithmic fashion. For ExxAC, the range is extended to 8 kHz.

Table 7 Spectral data products

ID	Burst mode	Quantities	Bins	Rate
44D	particle burst	any 4 signals from: V1-6, Exx, ExxAC, SCM, derived	16-64	1/16-8 S/s
44E	wave burst	same 4 as above	16-64	1/16-8 S/s

9 Conclusion

The Digital Fields Board is responsible for the digital signal processing for the THEMIS waves package. The processing is performed by field programmable gate arrays instead of using a dedicated processor, and consumes very little power. Many functions that have previously been implemented in analog electronics are performed digitally, resulting in significant power savings.

The data products produced by the DFB are extremely flexible. By using cascading filter banks, the same signal can be transmitted at a number of different rates in low-pass or band-pass filtered form, and with minimal processing. This strategy is efficient for satellites like THEMIS that have many different burst modes.

Spectral data are calculated using a Fast Fourier Transform. One of the unique features of the DFB is its ability to transform to a field-aligned coordinate system prior to calculating the wave spectra. This allows us to separate parallel and perpendicular components in the wave spectra.

The Digital Fields Board provides the digital processing necessary for observing waves in the electric and magnetic fields. All five DFBs have been turned on and checked out in-flight, and are functioning perfectly. We look forward to new and exciting science that can come from the DFB and all of the instruments on THEMIS.

References

Andraka R (1998) A survey of cordic algorithms for FPGAs. In: Proceedings of the 1998 ACM/SIGDA sixth international symposium on Field Programmable Gate Arrays, Feb. 22-24, 1998, Monterey, CA

Angelopoulos V (2008) The THEMIS mission. Space Sci Rev, this issue

Auster HU, Glassmeier KH, Magnes W, Aydogar O, Baumjohann W, Constantinescu D, Fischer D, Fornacon KH, Georgescu E, Harvey P, Hillenmaier O, Kroth R, Ludlam M, Narita Y, Nakamura R, Okrafka K, Plaschke F, Richter I, Schwarz H, Stoll B, Valavanoglou A, Wiedemann M (2008) The THEMIS fluxgate magnetometer. Space Sci Rev, this issue

Bonnell J, author2, author3 (2008) The Electric Field Instrument for THEMIS. Space Sci Rev, this issue

Press WH, Teukolsky SA, Vetterling WT, Flannery BP (1992) Numerical Recipes in C, 2nd edn. Cambridge University Press

Roux A, Le Contel O, Coillot C, Boubdellah A, de la Porte B, Alison D, Ruocco
    S, Vassal MC (2008) The Search Coil Magnetometer for THEMIS. Space Sci
    Rev, this issue
Taylor E, author2, author3 (2008) The Instrument Data Processing Unit for
    THEMIS. Space Sci Rev, this issue
Volder JE (1959) The CORDIC trigonometric computing technique. IRE Transac-
    tions on Electronic Computers